The Ndc80 complex uses a tripartite attachment point to couple microtubule depolymerization to chromosome movement

John G. Tooley, Stephanie A. Miller, and P. Todd Stukenberg
Department of Biochemistry and Molecular Genetics, University of Virginia Medical Center, Charlottesville, VA 22908

ABSTRACT **In kinetochores, the Ndc80 complex couples the energy in a depolymerizing microtubule to perform the work of moving chromosomes. The complex directly binds microtubules using an unstructured, positively charged N-terminal tail located on Hec1/Ndc80. Hec1/Ndc80 also contains a calponin homology domain (CHD) that increases its affinity for microtubules in vitro, yet whether it is required in cells and how the tail and CHD work together are critical unanswered questions. Human kinetochores containing Hec1/Ndc80 with point mutations in the CHD fail to align chromosomes or form productive microtubule attachments. Kinetochore architecture and spindle checkpoint protein recruitment are unaffected in these mutants, and the loss of CHD function cannot be rescued by removing Aurora B sites from the tail. The interaction between the Hec1/Ndc80 CHD and a microtubule is facilitated by positively charged amino acids on two separate regions of the CHD, and both are required for kinetochores to make stable attachments to microtubules. Chromosome congression in cells also requires positive charge on the Hec1 tail to facilitate microtubule contact. In vitro binding data suggest that charge on the tail regulates attachment by directly increasing microtubule affinity as well as driving cooperative binding of the CHD. These data argue that in vertebrates there is a tripartite attachment point facilitating the interaction between Hec1/Ndc80 and microtubules. We discuss how such a complex microtubule-binding interface may facilitate the coupling of depolymerization to chromosome movement.**

Monitoring Editor
David G. Drubin
University of California, Berkeley

Received: Jul 23, 2010
Revised: Feb 1, 2011
Accepted: Feb 8, 2011

INTRODUCTION

The kinetochore is a macromolecular machine assembled on centromeric chromatin during mitosis. Its predominant role is to anchor replicated DNA to spindle microtubules and to couple the energy of microtubule depolymerization to segregate sister chromatids. The kinetochore also regulates the dynamics of captured microtubules, corrects errors in microtubule attachment, and generates the spindle checkpoint, a fail-safe mechanism used by the cell to ensure that all chromosomes are properly attached to the mitotic spindle (Cleveland *et al.*, 2003; Santaguida and Musacchio, 2009).

The mammalian kinetochore is composed of more than 80 proteins, many of which are evolutionarily conserved (Cheeseman and Desai, 2008). The four-member Ndc80 complex, consisting of Ndc80 (Hec1 in humans), Nuf2, Spc24, and Spc25, is critical for kinetochore function (Wigge and Kilmartin, 2001; Deluca *et al.*, 2002, 2003; Martin-Lluesma *et al.*, 2002; McCleland *et al.*, 2003, 2004). At the kinetochore, the Ndc80 complex is closely associated with KNL-1 and the four-member Mis12 complex to form the "KMN network." This KMN supercomplex serves as the major attachment site for captured spindle microtubules (Cheeseman *et al.*, 2006). In all tested eukaryotic systems the Ndc80 complex directly binds microtubules, and loss of its activity results in failure by the kinetochore to bind microtubules and to congress chromosomes to form a metaphase plate (Cheeseman and Desai, 2008). In addition, mutant kinetochores cannot align chromosomes when they lack the unstructured tail of Hec1/Ndc80, which is critical for the complex to bind microtubules (Wei *et al.*, 2007; Ciferri *et al.*, 2008; Guimaraes *et al.*, 2008; Miller *et al.*, 2008). The Ndc80 complex can track on the plus end of a depolymerizing microtubule in vitro and can produce force while doing so (Powers *et al.*, 2009). Together these data argue that the

This article was published online ahead of print in MBoC in Press (http://www.molbiolcell.org/cgi/doi/10.1091/mbc.E10-07-0626) on February 16, 2011.

Address correspondence to: P. Todd Stukenberg (pts7h@virginia.edu).

Abbreviations used: ACA, anti-centromere antibodies; CD, circular dichroism; CHD, calponin homology domain; EGFP, enhanced green fluorescent protein; EM, electron microscopy; GAPD, glyceraldehyde-3-phosphate dehydrogenase; KNL-1, Kinetochore Null-1; WT, wild type.

Ndc80 complex directly binds microtubules to allow kinetochores to move chromosomes.

The N terminus of the Hec1/Ndc80 protein binds microtubules and contains a calponin homology domain (CHD) in addition to the 80-amino-acid unstructured tail (Wei *et al.*, 2007). The remainder of Hec1/Ndc80 forms a ~500Å coiled coil that dimerizes with Nuf2. Like Hec1/Ndc80, Nuf2 possesses a CHD at its N terminus (Ciferri *et al.*, 2008). The C termini of Hec1/Ndc80 and Nuf2 are joined to the N-terminal coils of Spc24 and Spc25 through a tetramerization domain (Maiolica *et al.*, 2007). In contrast to the more distal Hec1/Ndc80 and Nuf2, which point outward from the DNA, the globular C-terminal regions of Spc24 and Spc25 are oriented closer to the centromere (Wei *et al.*, 2005, 2006; Deluca *et al.*, 2006; Wan *et al.*, 2009).

To appreciate how kinetochores couple microtubule depolymerization energy to perform the work of moving chromosomes, it is critical to understand how the Ndc80 complex interacts with microtubules. Proteins often use a dual CHD to attach to actin filaments (Sjoblom *et al.*, 2008), and a dual CHD is essential for microtubule interactions by the plus-end tracking protein EB1/Bim1 (Hayashi and Ikura, 2003; Slep and Vale, 2007; Zimniak *et al.*, 2009). Similarly, the Hec1/Ndc80 CHD is incapable of binding microtubules on its own (Miller *et al.*, 2008) and must exist in the context of the Ndc80 complex for binding to occur. Both Hec1/Ndc80 and Nuf2 CHD mutants decrease the affinity of the complex for microtubules in vitro, but this binding defect is less severe than in mutants lacking the unstructured tail (Ciferri *et al.*, 2008). Cryo-electron microscopy (EM) images of recombinant Ndc80 complex bound to a microtubule reveal that a region of the Hec1/Ndc80 CHD—termed the "toe"—binds the surface of a microtubule at a discrete point between adjacent tubulin subunits (Alushin *et al.*, 2010). In addition, the Ndc80 complex has lower affinity for curved protofilaments compared with the lateral surface of microtubules. This lowered affinity suggests that the toe acts as a conformation sensor—allowing the Ndc80 complex to bind straight microtubules but causing release in response to protofilament curvature (Alushin *et al.*, 2010). Importantly, the role of the Hec1/Ndc80 CHD in vivo remains untested.

The unstructured tail of Hec1/Ndc80 is essential for kinetochore function in vertebrates (Guimaraes *et al.*, 2008; Miller *et al.*, 2008), and it has been proposed to have two functions. It can bind microtubules on its own in vitro and it increases the affinity of the dual CHD binding (Ciferri *et al.*, 2008; Miller *et al.*, 2008). The tail interaction requires the unstructured and negatively charged E-hooks on tubulin (Miller *et al.*, 2008). The Hec1/Ndc80 tail is highly positively charged, and phosphorylation of this motif by the Aurora kinases can decrease microtubule affinity (Cheeseman *et al.*, 2006; Ciferri *et al.*, 2008; Guimaraes *et al.*, 2008). In addition, the tail of Hec1/Ndc80 has been shown to facilitate cooperative microtubule binding of the Ndc80 complex in vitro (Cheeseman *et al.*, 2006; Ciferri *et al.*, 2008; Alushin *et al.*, 2010), and electron density that is presumed to be the tail residues facilitates tight packing of adjacent Ndc80 subunits along the surface of a microtubule. This tight packing along protofilaments suggests a model whereby tight affinity of the Ndc80 complex to microtubules would be generated by cooperative binding and that this could be released through the conformational changes that accompany depolymerization (Alushin *et al.*, 2010).

In this study, we use a knockdown and rescue system in human cells to examine the in vivo contribution of the Hec1/Ndc80 CHD and the unstructured tail to binding microtubules and congressing chromosomes. We demonstrate that mutants lacking positive charge in either the CHD or the unstructured tail severely compromise kinetochore function. Our data suggest that the Ndc80 complex couples microtubule depolymerization to chromosome movement using two microtubule-binding surfaces on the CHD which accurately position Ndc80 on a microtubule. Furthermore, the vertebrate Ndc80 complex relies on an unstructured tail to strengthen binding through charge-based interactions. Our data demonstrate the critical requirement of the toe region of the Hec1/Ndc80 CHD, consistent with this being a conformational sensor. Our data also suggest that the E-hooks of tubulin interact with both the CHD and the Hec1/Ndc80 tails to increase affinity for a microtubule through electrostatic interactions.

RESULTS

Cells expressing Hec1/Ndc80 CHD mutants assemble kinetochores properly

We measured the functions of three lysines (K89, K115, and K166) that reside in the highly basic region of the Hec1/Ndc80 CHD. Lys-166 is part of the toe region of Hec1/Ndc80 that docks near the tubulin dimer interface, and is proposed to be part of a microtubule conformation sensor (Alushin *et al.*, 2010). Lys-89 and Lys-115 reside close together but away from the Hec1/Ndc80 toe. These amino acids are located close to the predicted exit point of negatively charged tubulin E-hooks (Figure 1B) (Alushin *et al.*, 2010). Each lysine was first mutated to negatively charged glutamic acid. These mutations have been previously shown to create microtubule binding defects in vitro (Ciferri *et al.*, 2008). We examined the function of each of these lysines individually as well as mutated in pairs (K89/K115 and K89/K166) (Figure 1C). Before testing mutants in vivo, we confirmed that these point mutants do not grossly misfold the CHD in vitro. The study of Ndc80 function in vitro has been greatly enhanced by the generation of Ndc80^{bonsai} constructs, which are engineered to lack the coiled-coil domains (Ciferri *et al.*, 2008). A subset of the mutations was engineered into Ndc80^{bonsai} constructs and purified from *Escherichia coli,* and their circular dichroism (CD) spectrums and gel filtration profiles were compared with wild-type (WT) Ndc80^{bonsai}. CHD mutants yielded CD spectra or fractionation patterns similar to control Ndc80^{bonsai} complexes, demonstrating that the mutations do not greatly change the overall structure of the proteins (Supplemental Figure 1, A and B).

To ask whether Hec1/Ndc80 requires a functional CHD in cells, we used a knockdown and replacement protocol to measure the function of kinetochores during the first mitosis during which cells contain mutated proteins (Miller *et al.*, 2008). HeLa cells were synchronized using a double thymidine block. Endogenous Hec1/Ndc80 protein was removed using transfected siRNA oligos and replaced by cotransfection of a rescue plasmid encoding an siRNA-resistant Hec1/Ndc80 gene (Figure 1A). Cells were fixed 8–12 h after thymidine release, and rescued cells were identified by an enhanced green fluorescent protein (EGFP) tag engineered onto the C terminus of Hec1/Ndc80. Immunoblots demonstrated efficient knockdown of the endogenous protein concomitant with the expression of GFP-tagged Hec1 (Supplemental Figure 2A). Nearly all WT rescued metaphase cells (as judged by DAPI staining) also expressed EGFP, further demonstrating the efficiency of our system (Supplemental Figure 2B). Immunofluorescence with anti-Hec1/Ndc80 antibodies confirmed that Hec1/Ndc80 intensity levels were similar to endogenous concentrations in our rescued cells (Supplemental Figure 2C). We also used immunofluorescence to confirm that kinetochores are properly assembled (Supplemental Figure 3). In Hec1/Ndc80 knockdown cells, Hec1/Ndc80, Spc25, and CENP-E are largely absent from kinetochores, and BubR1 is present but at reduced levels. The more centromere proximal KNL-1 (kinetochore) and ACA (centromere) signals are present in

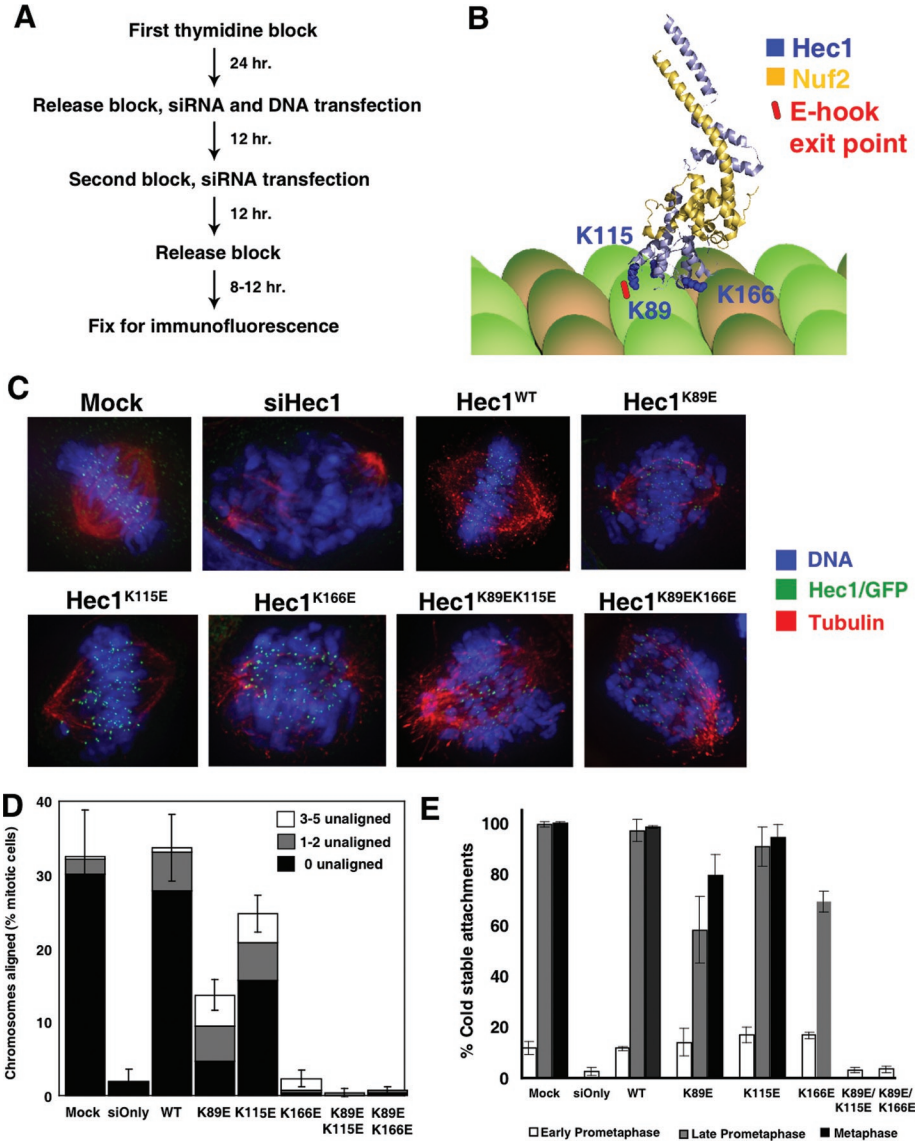

FIGURE 1: The CHD of Hec1/Ndc80 is essential for congression of chromosomes to the metaphase plate. (A) Scheme used to visualize the first mitotic division after endogenous Hec1/Ndc80 is replaced by exogenous Hec1/Ndc80 in synchronized HeLa cells. (B) Ribbon diagram depicting the N-terminal CHD regions of Hec1/Ndc80 (light blue, amino acids 80–285) and Nuf2 (yellow, amino acids 4–169). Lysine residues altered in mutants are shown in dark blue. The predicted exit point of a tubulin E-hook is indicated in red. Diagram was constructed based on the crystal structure of Ndc80^{bonsai} (Cifferi *et al.*, 2008) bound to a microtubule (Alushin *et al.*, 2010). (C) Representative images of the predominant mitotic figures from siHec1 knockdown and rescued cells that have been stained for Hec1/Ndc80 (green), tubulin (red), and DNA (blue). WT and CHD mutant cells are identified by an expressed EGFP, and are costained for tubulin and DNA. For mock treated, Hec1^{WT}, Hec1^{K89E}, and Hec1^{K115E} cells, representative metaphase images are shown. For siHec1(siOnly), Hec1^{K166E}, Hec1$^{K89E/K115E}$, and Hec1$^{K89E/K166E}$, prometaphase cells are shown. (D) Mitotic cells were scored for chromosome alignment into a metaphase plate, and the percentage of metaphase cells was plotted. Metaphase cells were further subdivided to indicate cells with all chromosomes aligned (black), cells with one to two unaligned chromosomes (gray), and cells with three to five unaligned chromosomes (white). N = 3; 100 cells per experiment. Error bars = SD of total metaphase cell population. (E) Cells were incubated in ice-cold medium prior to fixation and immunostaining. Ten sister kinetochores from 5–10 cells (N = 3) were scored for kinetochore-embedded microtubules, and the mean percentage was plotted. Error bars = SD.

knockdown cells. In Hec1^{WT}, Hec1$^{K89E/K1115E}$, and Hec1$^{K89E/K166E}$ cells, all proteins localized to kinetochores. We conclude that kinetochores assemble properly after knockdown of the endogenous Hec1/Ndc80 and replacement with our CHD mutants.

Kinetochores require the Hec1/Ndc80 CHD to bind microtubules

We tested whether kinetochores containing Hec1/Ndc80 CHD mutants could properly align chromosomes in vivo. Cells were fixed and stained for tubulin and DNA. Mock transfected and Hec1/Ndc80 knockdown cells were also stained with anti-Hec1/Ndc80 antibodies, and Hec1/Ndc80 in rescued cells was identified with anti-GFP antibodies. Cells were scored for their ability to congress chromosomes to form a metaphase plate. Metaphase was defined as the majority of chromosomes in the center of the cell (more than five unaligned were scored as late prometaphase), although the pole-to-pole width of the plate varied greatly. In mock transfected and Hec1^{WT} cells, more than 30% of mitotic cells were able to achieve proper chromosome alignment at the time of fixation (Figure 1, C and D). Only 2% of the mitotic cells were able to form a metaphase plate after Hec1/Ndc80 siRNA treatment and rescue with an empty EGFP-expressing plasmid, consistent with published results (Guimaraes *et al.*, 2008; Miller *et al.*, 2008). Replacement of endogenous Hec1/Ndc80 with either double mutant resulted in an alignment defect identical to removing the entire protein. Similarly, only 2.3 ± 1.2% of Hec1^{K166E} cells contained aligned chromosomes, demonstrating that Lys-166 is a critical residue for Hec1/Ndc80 function in vivo.

We identified intermediate phenotypes in the K115E and K89E mutants, which bind microtubules near the predicted exit point of tubulin E-hooks (Alushin *et al.*, 2010). Hec1^{K115E} mutant cells were able to largely restore metaphase alignment, with 24.7 ± 2.5% of mitotic cells scored as aligned (Figure 1, C and D). Cells expressing the Hec1^{K89E} mutant had a more severe phenotype, with 13.7 ± 2.1% of cells scored as aligned. In addition to lower percentages of metaphase cells compared with controls, we saw additional spindle defects in these cells. First, although 5.3% of Hec1^{WT}-expressing cells are found in anaphase, we could not identify any CHD mutant cells in anaphase. This finding suggests that cells containing CHD mutants either cannot bind chromosomes well enough to fulfill the spindle checkpoint or cannot segregate chromosomes in anaphase. We found that an informative way to measure more subtle alignment defects was to identify cells with metaphase plates and quantify the number of chromosomes that remain at or near the poles (Figure 1D). In the mock treated conditions or in cells rescued with Hec1^{WT}, more than 82% of metaphase cells had all their chromosomes

aligned at the center. In contrast, 67% of Hec1^{K89E} and 35% of Hec1^{K115E} metaphase cells had unaligned chromosomes. We conclude that the K115E and K89E mutants have similar intermediate phenotypes and note that the double mutant is more severe. This information suggests that these two residues share a common function.

After kinetochores generate bipolar attachments, they use the bound microtubules to generate force and pull sisters apart (Maddox *et al.*, 2003). The distance between sisters (interkinetochore distance) can be used as a readout of the forces generated. In early prometaphase cells, which presumably have few kinetochore–microtubule attachments, all of the cell populations were similar to nocodazole-treated cells (0.68 ± 0.01 μm) (Supplemental Figure 4A). CHD double point mutant cells remained in early prometaphase and could not separate sister chromatids. Hec1^{K89E} (1.11 ± 0.04 μm) and Hec1^{K115E} (1.21 ± 0.02 μm) cells in metaphase generated intermediate interkinetochore distances that were reduced compared with mock or Hec1^{WT} metaphase cells (1.40 ± 0.08 μm and 1.36 ± 0.04 μm, respectively). A percentage of Hec1^{K166E} cells were also able to progress to late prometaphase, and these cells had an average interkinetochore distance of 1.01 ± 0.04 μm. Therefore kinetochores from CHD mutant cells cannot effectively use microtubules to generate maximal pulling forces on sister kinetochores. Like the alignment defects, there is a gradation in these phenotypes, with Hec1^{K166E} cells able to generate the least amount of force and Hec1^{K115E} cells showing the smallest diminishment of force production.

Kinetochore–microtubule attachments are resistant to cold temperature, a treatment that depolymerizes most microtubules in a mitotic cell (Brinkley and Cartwright, 1975). Control and CHD mutant cells were incubated in ice-cold medium prior to fixation and stained for tubulin, Hec1/Ndc80 (or GFP), and ACA (see images in Supplemental Figure 5). The percentage of kinetochores with embedded cold-stable microtubule bundles (K-fibers) was scored. The double mutants acted almost identically to a Hec1/Ndc80 knockdown cell, and the single mutants generated a gradation of phenotypes. Hec1^{K115E} and Hec1^{K89E} mutant cells generated cold-stable attachments at 94.0 ± 5.3% and 79.3 ± 8.1% of kinetochores during metaphase, demonstrating that most kinetochores containing these mutants are able to bind microtubules. Interestingly, 69.3 ± 4.2% of Hec1^{K166E} cells had cold-stable attachments in metaphase. This finding demonstrates that these kinetochores were able to bind microtubules at reduced levels but cannot use the attachments to align chromosomes.

In conclusion, all three CHD residues that we tested play important roles in generating tension and aligning chromosomes, although kinetochores containing the single mutants appear able to attach microtubules with some efficiency. All three residues make independent contributions to kinetochore function, as double mutants are more severe and cannot stabilize microtubules against cold-induced depolymerization.

CHD mutant phenotypes cannot be rescued by inhibiting Aurora B phosphorylation of the Hec1/Ndc80 tail

Phosphorylation of the Hec1/Ndc80 N-terminal tail by Aurora B lowers its affinity for microtubules in vitro and is believed to be a critical step for kinetochores to release improper attachments in vivo (Cheeseman *et al.*, 2006; Ciferri *et al.*, 2008; Guimaraes *et al.*, 2008; Alushin *et al.*, 2010; Welburn *et al.*, 2010). Therefore we wondered whether the reason our CHD mutants were not aligning chromosomes is because they trigger phosphorylation of the Hec1/Ndc80 tail. Phosphorylation would presumably weaken kinetochore interactions with microtubules and indirectly cause the phenotypes we observe. To test this hypothesis, we generated a trio of Hec1/Ndc80 CHD mutants that also has nine consensus Aurora B phosphorylation sites on the tail mutated to alanine (Hec1$^{9A/K89E}$, Hec1$^{9A/K166E}$, Hec1$^{9A/K89EK166E}$) (sites highlighted in Figure 2A). As a control for the role of phosphorylation, we created a phospho-null mutant (Hec1^{9A}) that contains the nine mutated phosphorylation sites but lacks mutations in the CHD.

HeLa cells can generate productive microtubule attachments, generate interkinetochore tension, and align chromosomes after knockdown and replacement with Hec1^{9A} mutants (Figure 2, B and C). We did notice a slight increase in unaligned chromosomes in our Hec1^{9A} cells as well as an increase in interkinetochore distance (Supplemental Figure 4B), in agreement with published data (Deluca *et al.*, 2006). The Hec1$^{9A/K89E/K166E}$ mutant cells, however, produced a phenotype that recapitulated the Hec1$^{K89E/K166E}$ mutant. Only 0.3 ± 0.6% of these mutant cells had metaphase-aligned chromosomes (Figure 2, B and C). Furthermore, they could not generate a stretch between sister kinetochores (Supplemental Figure 4B) and could not stabilize microtubules against cold-induced depolymerization (Figure 2D). We conclude that kinetochores cannot generate K-fibers using tail interactions alone, but they require a functional CHD.

In contrast, the phenotypes generated in our Hec1^{K89E} and Hec1^{K166E} cells were improved by removing Aurora sites from the Hec1/Ndc80 tail. Approximately twice as many Hec1$^{9A/K89E}$ mitotic cells formed a metaphase plate than did Hec1^{K89E} cells (compare Figure 1D with Figure 2C). In addition, Hec1$^{9A/K89E}$ metaphase cells had a similar number of stabilized microtubules compared with Hec1^{WT} and Hec1^{9A} controls (Figure 2D), although there was less rescue of their ability to generate forces to separate sister kinetochores (Supplemental Figure 4B). Creating an unphosphorylated tail also partially rescued the Hec1^{K166E} mutation (Figure 2 and Supplemental Figure 4B); but here again the 9A/K166E mutation was more severe than the 9A/K89E. We conclude that Aurora B phosphorylation of the Hec1/Ndc80 tail does contribute to the intermediate phenotypes we see in our single mutants, but the main reason for the phenotype is impaired interaction between the Hec1/Ndc80 CHD and a microtubule.

Both the Hec1/Ndc80 CHD and the N-terminal tail use charge to interact with microtubules

Phenotypes resulting from lysine mutation could be due to loss of positive charge or loss of posttranslational modifications on the lysine. To distinguish between these models we tested the contribution of charge. Mutants were generated that replaced a pair of lysines in the CHD with glutamic acid (Hec1$^{K89E/K166E}$), alanine (Hec1$^{K89A/K166A}$), or arginine (Hec1$^{K89R/K166R}$). Whereas Hec1$^{K89R/K166R}$ mutant cells (which retained the charge state) were able to restore metaphase alignment, neither Hec1$^{K89A/K166A}$- nor Hec1$^{K89E/K166E}$-expressing cells could align chromosomes to form a metaphase plate (Figure 3, A and B). In contrast, Hec1$^{K89R/K166R}$ cells could progress into anaphase (unpublished data), generate sufficient interkinetochore tension (Supplemental Figure 4C), and stabilize microtubules against cold-induced depolymerization (Figure 3C). We conclude that positive charge in the side chains of these amino acids is critical for kinetochore function.

Although Hec1$^{K89A/K166A}$ mutant cells could not align chromosomes efficiently enough to form a metaphase plate, some chromosomes formed cold-stable attachments and generated interkinetochore tension at reduced levels. No such attachments

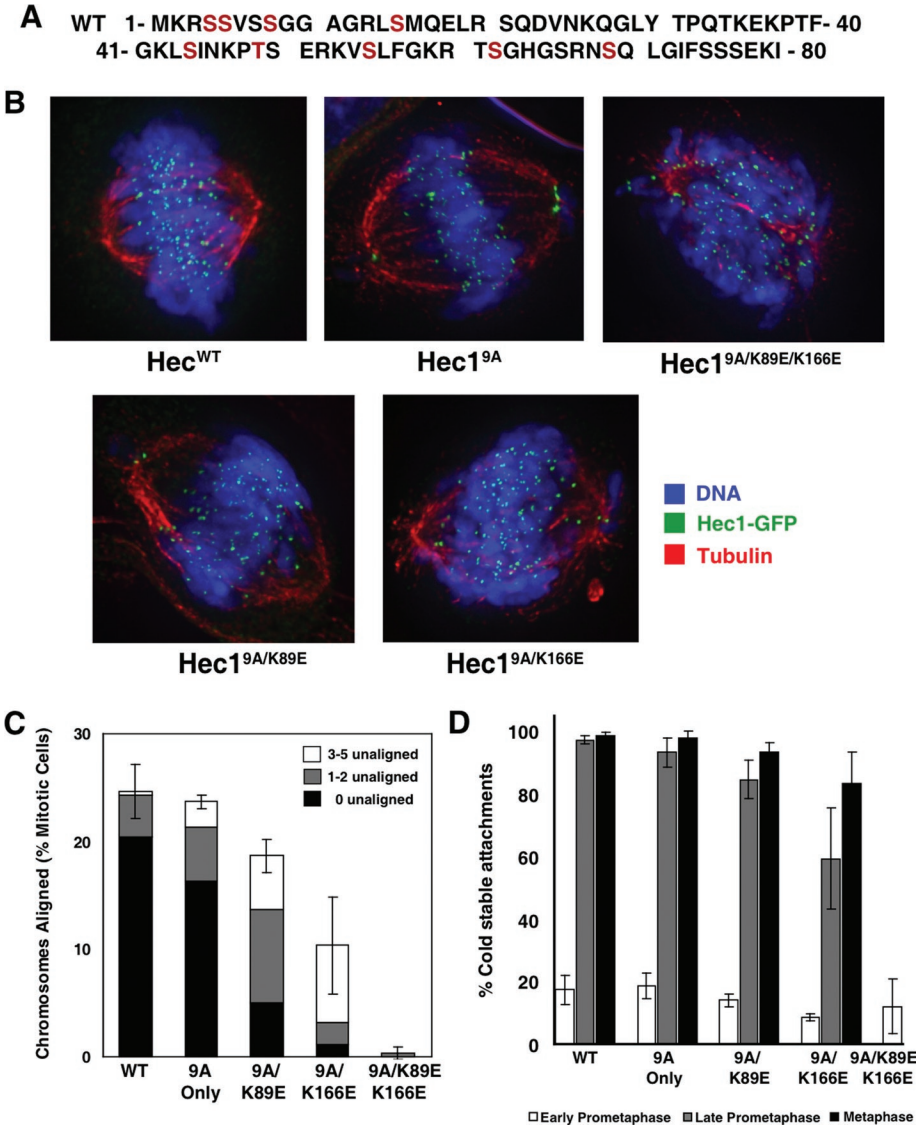

FIGURE 2: Hec1/Ndc80 CHD mutant phenotypes cannot be rescued by preventing Aurora phosphorylation of the Hec1/Ndc80 tail. (A) Sequence of the 80-amino-acid Hec1/Ndc80 tail region. Nine WT residues were mutated to alanine (Hec1^{9A}) and are indicated in red. (B) Representative images of predominant mitotic figures from siHec1 knockdown and rescued cells that have been stained for Hec1/Ndc80, tubulin, and DNA. For Hec1^{WT}, Hec1^{9A}, Hec1$^{9A/K89E}$, and Hec1$^{9A/K166E}$, metaphase images are shown. For Hec1$^{9A/K89E/K166E}$, only prometaphase cells are observed. (C) Rescued mitotic cells were stained for tubulin and DNA, identified by an EGFP kinetochore signal, and scored for chromosome alignment. The percentage of metaphase-aligned cells was plotted in comparison to mock transfected cells. N = 3; ≥100 cells per experiment. Metaphase cells were further subdivided to indicate cells with all chromosomes aligned (black), cells with one to two unaligned chromosomes (gray), and cells with three to five unaligned chromosomes (white). Error bars = SD of total metaphase cell population. (D) Cells were incubated in ice-cold medium prior to fixation and immunostaining with tubulin and ACA antibodies. Ten kinetochores in 5–10 cells (N = 3) were scored for percentage of kinetochores containing embedded microtubules, and the mean percentage was plotted. Error bars = SD.

were seen in the Hec1$^{K89E/K166E}$-expressing cells (Figure 3C and Supplemental Figure 4C). These data demonstrate a gradation of phenotypes as the positively charged lysines in the CHD are replaced with positive, neutral, and negatively charged residues.

A Hec1/Ndc80 mutant lacking the N-terminal tail region (Hec1$^{\Delta N}$) is unable to align chromosomes in vivo (Guimaraes *et al.*, 2008; Miller *et al.*, 2008). This 80-amino-acid region contains 15 positively charged and 5 negatively charged residues spread across its length. To test the contribution of charge to Hec1/Ndc80 tail binding to microtubules, we tested a charge-neutral protein (Hec1^{NEU}) where 10 positively charged residues were mutated to alanine (Figure 4A). These mutations reduce the net charge of the tail from +10 to 0. A portion of recombinant Hec1^{NEU} migrated as a higher molecular weight species in gel filtration, suggesting that charge on the tail may regulate oligomeric state in vitro (Supplemental Figure 1). This protein also lost much of its ability to bind microtubules in vitro (Figure 4B and Supplemental Figure 7). While charge-neutral Ndc80^{bonsai} pelleted better than WT at lower microtubule concentrations, the binding curve reached a plateau and never exceeded 34.9% bound—demonstrating that charge on the N-terminal tail of Hec1/Ndc80 stabilizes the interaction between the Ndc80 complex and microtubules.

The Hec1^{NEU} mutant was tested in vivo using our knockdown and replacement protocol. Hec1^{NEU} mutant cells were unable to align chromosomes and form a metaphase plate (Figure 4, C and D). Hec1^{NEU} mutant cells remained in early prometaphase with few (14.9 ± 1.2%) cold-stable microtubules (Figure 4E) and kinetochores that were unable to generate forces to stretch sisters apart (average interkinetochore distance of 0.79 ± 0.07 μm) (Figure 4F). Kinetochore assembly was unperturbed in Hec1^{NEU} mutant cells (Supplemental Figure 6). Therefore the charge on the N-terminal unstructured region of Hec1/Ndc80 is critical for kinetochores to bind microtubules and align chromosomes.

DISCUSSION

Our data provide significant insight into the mechanism by which vertebrate kinetochores couple conformational changes generated by microtubule depolymerization into the energy to move chromosomes. Like the unstructured N-terminal tail, the CHD of Hec1/Ndc80 is essential for binding microtubules and congressing chromosomes in vivo. Hec1/Ndc80 knockdown cells rescued with CHD point mutants fail to align chromosomes, generate tension across sister kinetochores, or produce stable microtubule attachments. Interactions with microtubules are mediated by charge, because lysines can be functionally replaced by arginines, but not by alanines or glutamic acids. We also extend our studies of the Hec1/Ndc80 tail by demonstrating that the large amounts of positive charge residing in this unstructured region drive proper kinetochore function. A formal possibility was that the CHD phenotypes we observed were indirectly caused by activation of the microtubule release system, which includes Aurora B phosphorylation of the tail of Hec1/Ndc80

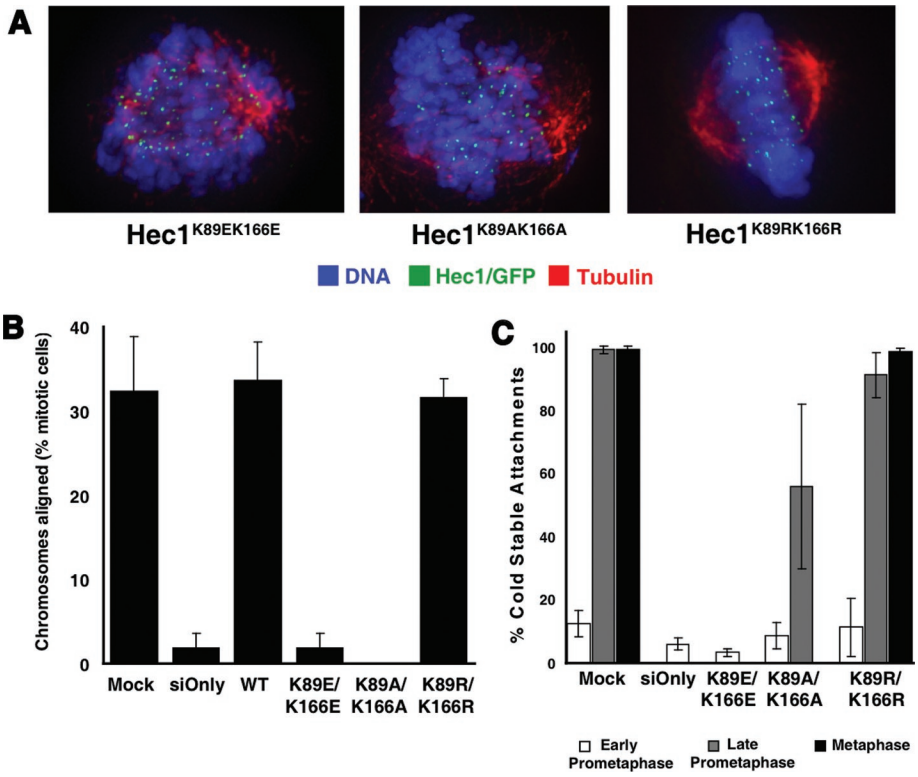

FIGURE 3: The interaction between the Hec1/Ndc80 CHD and a microtubule requires charge. (A) Representative images of the predominant phenotype of Hec1/Ndc80 CHD mutant cells. For Hec1$^{K89E/K166E}$ mutant cells, only early prometaphase figures were found. Both early prometaphase and late prometaphase (shown) figures were found in Hec1$^{K89A/K166A}$ mutant cells. For Hec1$^{K89R/K166R}$ mutant cells, both prometaphase and metaphase (shown) figures were observed. (B) Mitotic cells were scored for chromosome alignment, and the percentage of metaphase-aligned cells was plotted. N = 3; ≥100 cells counted in each experiment. (C) Cells were incubated in ice-cold medium prior to fixation and immunostaining with tubulin and ACA antibodies. Mock treated and siHec1 knockdown cells also were stained for Hec1/Ndc80 (9G3). Ten kinetochores in 5–10 cells (N = 3) were scored for the percentage of kinetochores containing embedded microtubules, and the mean percentage was plotted. Error bars = SD.

and additional KMN components (Welburn *et al.*, 2010). We tested this possibility by combining mutations in both the CHD and regulatory sites in the tail, and although there may be some triggering of the release system, our data suggest a direct role for the CHD binding to the microtubule in chromosome congression. We conclude that electrostatic contacts dictate the interaction between Hec1 and a microtubule in vivo. This interaction is dependent on the two positively charged regions of the Hec1/Ndc80 CHD and is facilitated by additional electrostatic interactions on the tail.

The Hec1/Ndc80 CHD has two distinct microtubule-binding motifs in vitro, and both are required in vivo

We have demonstrated that three lysine residues implicated in microtubule binding in vitro (Ciferri *et al.*, 2008) are critical for kinetochore function in vivo. The recent publication of a high-resolution cryo-EM structure of the Ndc80^{bonsai} on microtubules provided significant insight into Ndc80 function (Alushin *et al.*, 2010) and allowed us to greatly refine the interpretation of our work. The residues that generated phenotypes are located in two distinct regions of the Hec1/Ndc80 CHD. In the crystal structure of Ndc80^{bonsai}, Lys-166 resides in the toe portion of the CHD that positions the Ndc80 complex at the interface between tubulin dimers and is proposed to work as a microtubule conformation sensor (Alushin *et al.*, 2010). It is also located adjacent to the Ser-165 residue, which is proposed to be a site of Nek2A regulation (Du *et al.*, 2008). In contrast, Lys-89 and Lys-115 reside away from the toe region of Hec1/Ndc80 but close to the predicted exit point for negatively charged E-hooks (Alushin *et al.*, 2010). As tubulin tails were too unstructured to be captured in the structural data, we cannot definitively say that lysines directly contact E-hooks. We note, however, that the closest negatively charged group emanating from the folded portion of a tubulin subunit is more than 10 Å from either Lys-89 or Lys-115. This finding strongly suggests that these CHD residues are in contact with E-hooks, and not the structured tubulin subunit. Thus our in vivo data strongly support the findings and many of the interpretations of the recent cryo-EM structure.

When we mutate each of these three residues alone we find that mutation of Lys-166 generates the most severe phenotype, demonstrating that the toe region of Hec1/Ndc80 is critical for proper kinetochore function in vivo. Mutation of Lys-89 or Lys-115 alone generates more intermediate phenotypes, whereas mutating these two residues in tandem is far more severe. These data could be interpreted in two ways. One interpretation is that Lys-89 and Lys-115 are both implicated in binding E-hooks, and in the absence of one contact point the other is able to maintain a certain level of contact with this region of a microtubule. When both contact points are lost, however, the Hec1/Ndc80 CHD is now unable to interact with E-hooks and all microtubule binding is lost. Alternatively, a genetic argument could be made that each of these residues has an independent function. We note that E-hooks have ~10–12 acidic residues (Hiser *et al.*, 2006), and both Lys-89 and Lys-115 lie close to the predicted E-hook emergence point. As there are no other nearby amino acids from the structured tubulin subunit to generate salt bridges, we propose a model where both Lys-89 and Lys-115 simultaneously interact with different glutamic acids on a single E-hook (Figure 5).

Role of the unstructured Hec1/Ndc80 tail

In vertebrates the Hec1/Ndc80 tail is required for kinetochore function in vivo (Guimaraes *et al.*, 2008; Miller *et al.*, 2008). The in vivo alignment phenotype we see in our paired CHD point mutants (where the tail is intact) is just as dramatic, however, as removing the entire tail or eliminating its positive charge. Thus both the CHD and the tail are absolutely essential. The role for the tail remains somewhat unclear, however. The Hec1 tail binds microtubules better than the CHD does in vitro, and it greatly increases the affinity of the dual CHD for microtubules. Our chargeless tail mutant reduces binding to microtubules in vitro and in vivo, strongly suggesting that additional microtubule contact by the tail facilitates binding. There is an alternative model, however, suggested by the recent cryo-EM data—that the tail controls cooperative binding. This model is also supported by our data, and we will discuss this later in this article. Finally, the tail is a point of regulation by the Aurora B kinase—suggesting an additional role for this 80-amino-acid region.

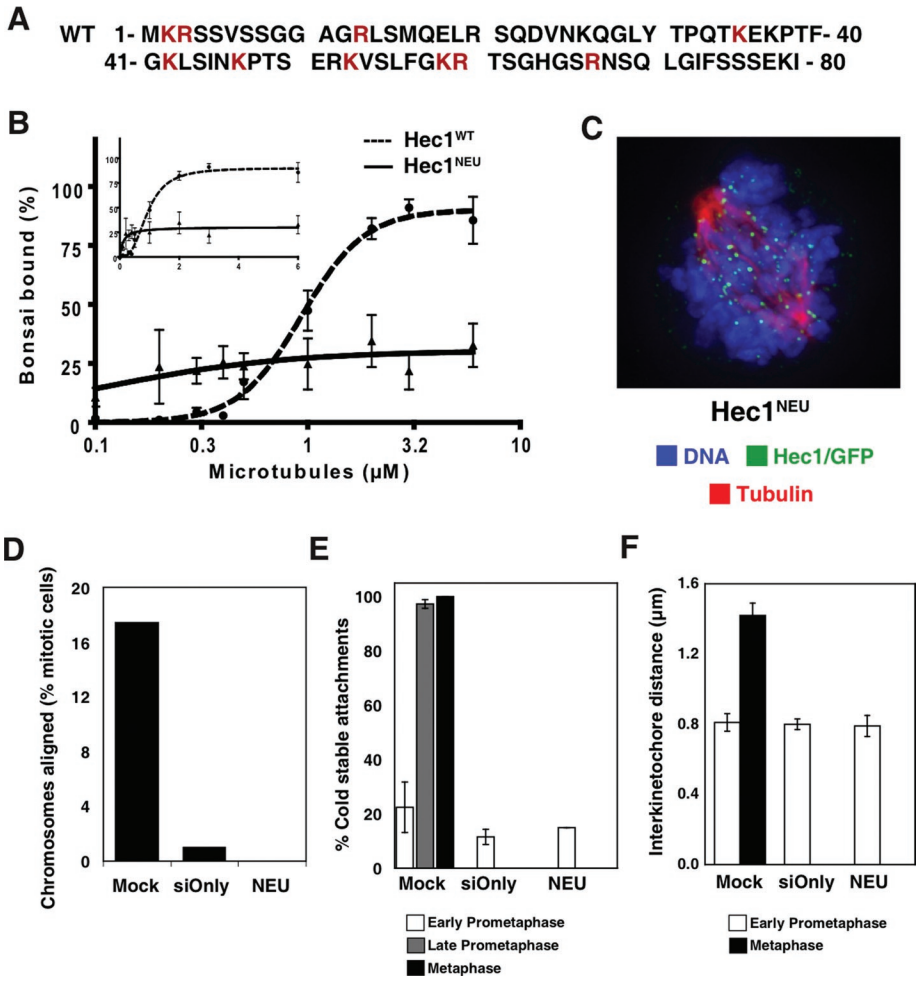

FIGURE 4: Positive charge in unstructured Hec1/Ndc80 tail is required for microtubule binding and chromosome congression. (A) Amino acid sequence of charge-neutral tail Hec1 mutant with mutated residues indicated in red. (B) WT and charge-neutral Hec1 tail Ndc80^{bonsai} were sedimented with the indicated concentrations of microtubules, and pellet samples (N = 3) were subjected to Western blotting with anti-hSpc25 antibody. Signal intensities were quantified, and the mean percentage of Ndc80^{bonsai} bound at each microtubule concentration was plotted on a log and linear scale (inset). For representative primary data, see Supplemental Figure 7. Error bars = SD. (C) Representative image of a knocked down cell that has been rescued with Hec1^{NEU}. The cell is stained for Hec1/Ndc80 (green), tubulin (red), and DNA (blue). In this condition only early prometaphase figures are found. (D) Mitotic cells were scored for kinetochore alignment (N ≥ 100), and the percentage of mitotic cells with aligned chromosomes was plotted. (E) Ten kinetochores from five or more cells (N > 50) were scored for kinetochore-associated microtubules (N = 2), and the mean percentage in early prometaphase, late prometaphase, and metaphase was plotted. (F) Ten sister kinetochores in at least five cells (N > 50) were identified by ACA staining between Hec1/Ndc80 signals, and the distance between those sister kinetochores was measured (N = 3). The mean distance is plotted for early prometaphase and metaphase cells. Error bars = SD.

The Ndc80 complex binds microtubules in patches in vitro (Ciferri *et al.*, 2008; Alushin *et al.*, 2010), suggesting that there is a preference for an Ndc80 complex to bind to a tubulin subunit adjacent to another bound Ndc80 complex. The cryo-EM data show that Ndc80 complexes tightly pack along a protofilament and there is a significant binding interface between adjacent Ndc80 complexes. These data suggest a treadmill model for Ndc80 function, where binding of multiple Ndc80 subunits along a tubulin protofilament generates a tighter binding surface. As an Ndc80 complex is released from a tubulin subunit following depolymerization-induced protofilament curvature, rebinding of that released subunit behind the last bound Ndc80 could allow a treadmilling mechanism that would provide the kinetochore with a tight binding interface that can also move with a depolymerizing microtubule. Although most of the density in the cryo-EM structure could be accounted for by the current crystal structure of a monomeric Ndc80^{bonsai} complex that lacks the unstructured tail, there was extra density between adjacent Ndc80 subunits when the WT complex was used that could represent the tail region of Hec1/Ndc80. This finding suggests a role for the tail in driving tight packing of adjacent Ndc80 proteins along a protofilament, in support of the model discussed earlier in the text (Figure 5A).

We also postulate an alternative role for the vertebrate Hec1/Ndc80 tail based on our previous in vitro finding that the tail binds microtubules on its own and even shows significant cooperative binding in the absence of a Hec1/Ndc80 CHD (Miller *et al.*, 2008). We propose that the tail may act as a tether to provide additional binding affinity following transient loss of CHD binding during periods of microtubule depolymerization. This tethering activity would allow an Ndc80 complex to move from one tubulin subunit to another (Figure 5B). Because our Hec1^{NEU} loses both overall binding and cooperative binding (which is presumably reflective of the tight packing of subunits), our data currently support either model. We note that the two models are not mutually exclusive, and we currently favor a model where both are correct. The Hec1/Ndc80 tail is 80 amino acids long, and assuming the tight packing model is correct we would estimate that <30 amino acids could be fit into the extra density identified by the cryo-EM structure, which would allow most of the tail to still act as a tether where it could both enhance microtubule binding affinity and facilitate the poleward transfer of an Ndc80 complex from a curvature-enacted release point (Figure 5B). It remains unclear how an exclusive role for the tail in packing Hec1/Ndc80 complexes would allow for the observed oscillations of chromosomes at the metaphase plate, where kinetochores must reposition themselves on polymerizing microtubules. Additionally, we speculate that intermediate amounts of Aurora B phosphorylation of the Hec1/Ndc80 tail could trigger a switch between a packing function and a tethering function. It is likely that an intermediate phosphorylation state would exist in prometaphase before kinetochore forces pull sister kinetochores apart. Clearly, these are all important areas for future research.

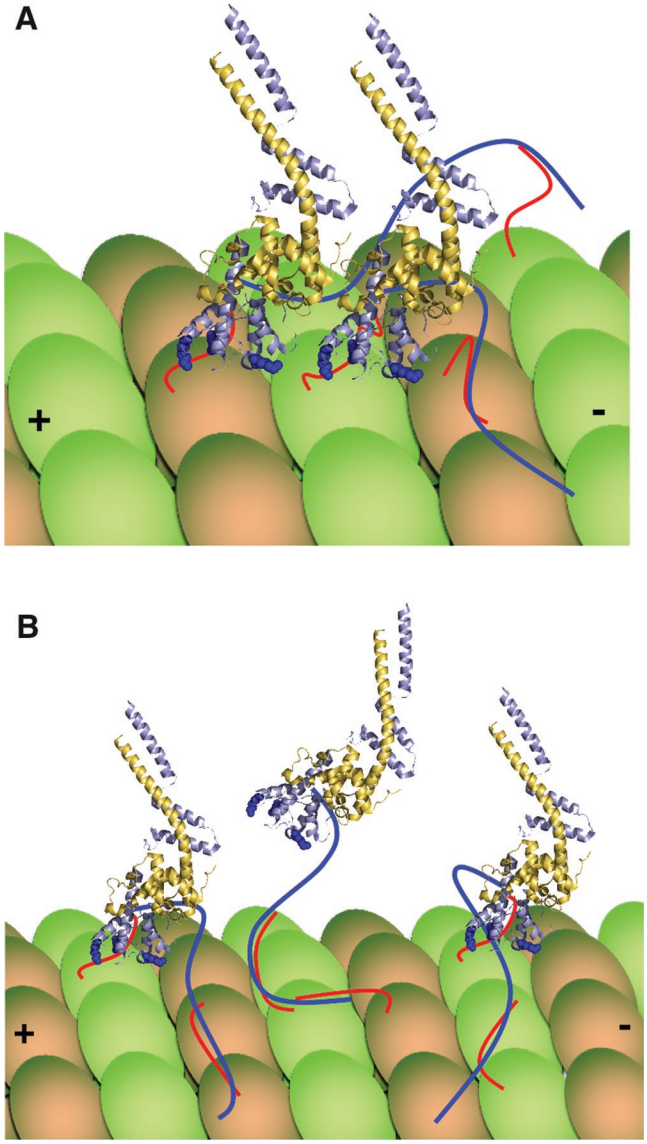

FIGURE 5: Model for vertebrate Hec1/Ndc80's interaction with a microtubule. (A) The unstructured tail of Hec1/Ndc80 (dark blue line) binds tubulin tails (red lines) and also acts to pack adjacent Ndc80 complexes on the surface of a microtubule. Lys-166 of the Hec1/Ndc80 CHD is a critical residue in the toe region of the protein, whereas tubulin E-hooks also interact with Lys-89 and Lys-115 of the Hec1/Ndc80 CHD (Alushin *et al.*, 2010). (B) Alternatively, the tail may function primarily to tether the Ndc80 complex to microtubules during periods when CHD binding is lost. The models depicted in (A) and (B) need not be mutually exclusive and could be regulated by Aurora phosphorylation of the Hec1/Ndc80 tail. For simplicity, only tubulin tails involved in binding are depicted.

MATERIALS AND METHODS

Cloning of Hec1 constructs

To facilitate cloning of mutants, the pGEX6P-2rbs WT human Ndc80^{bonsai} construct (a gift from A. Musacchio, IFOM-IEO Campus) was modified by placing an Fse1 restriction site prior to the N terminus of the Hec1/Spc25 fusion. Ndc80^{bonsai} CHD mutants were generated using two-step PCR mutagenesis. The charge-neutral tail mutant was generated by removing the WT tail and inserting a duplexed oligo coding for the Hec1/Ndc80 tail that contained the following 10 residues mutated to alanine: K2, R3, R13, K35, K42, K47, K53, K59, R60, and R67. For cell culture experiments, the first 84 amino acids of WT-Hec1 were cut from the Ndc80^{bonsai} using Fse1 and PpuM1 and subcloned into the FLAG-Hec1 rescue vector (Miller *et al.*, 2008) at these restriction sites. For CHD rescue experiments, WT-Hec1 containing the Fse1 restriction site was moved from the FLAG rescue vector into the pEGFP-N1 vector by using the Fse1 and Pst1 restriction sites. Mutants were cloned into EGFP rescue vectors either by moving them from the Ndc80^{bonsai} construct through FLAG-Hec1 into pEGFP-N1 using the restriction sites listed earlier in the text or by mutating the WT Hec1-EGFP construct using two-step PCR mutagenesis. For the Hec1^{9A} and Hec1$^{9A/CHD}$ mutant constructs, the following residues in the Hec1/Ndc80 tail were mutated to alanine: S4, S5, S8, S15, S44, T49, S55, S62, and S69. All constructs generated were verified by sequencing.

Recombinant protein expression and purification

To create the Hec1^{NEU} and Hec1$^{K89E/K115E}$ mutants, the bicistronic plasmid that expresses human Ndc80^{bonsai} was modified to fuse a 6-His tag to the N terminus of Hec1. 6-His Ndc80^{bonsai} was expressed, GST-purified, and cleaved with PreCission Protease (GE Healthcare Life Sciences, Piscataway, NJ) as described (Ciferri *et al.*, 2008). Cleaved recombinant protein was further purified using Ni-NTA agarose (Qiagen, Valencia, CA). Hec^{WT}, Hec1$^{\Delta N}$, and Hec1^{K166E} lack the 6-His tag and were purified as described (Ciferri *et al.*, 2008). Purified protein was dialyzed using a Slide-A-Lyzer Dialysis Unit (Thermo Fisher Scientific, St. Charles, MO) into dilution buffer (100 mM KCl, 10 mM Na-HEPES, 1 mM EDTA, 1 mM dithiothreitol, 1 mM $MgCl_2$, 0.1 M $CaCl_2$, 10% glycerol). Gel filtration was performed on a Superdex 200 column (GE Healthcare Life Sciences).

Microtubule polymerization

Phosphocellulose-purified bovine tubulin was polymerized to microtubules using Taxol (paclitaxel; Sigma, St. Louis, MO) as previously described (Desai *et al.*, 1999). Microtubules were resuspended in dilution buffer supplemented with an equimolar concentration of Taxol (20–40 μM).

Western blotting and microtubule cosedimentation assays

For determining microtubule binding and Hec1/Ndc80 knockdown levels, Western blotting was performed as previously described (McCleland *et al.*, 2004). For Hec1/Ndc80 knockdown, protein levels were determined by using anti-Hec1/Ndc80 9G3 antibody (GeneTex, Irvine, CA) at 1:2000 vol/vol. Cosedimentation assays were performed using Taxol-stabilized microtubules in dilution buffer and 20 μM Taxol as previously described (Cheeseman *et al.*, 2006). Protein was detected using anti-hSpc25 (1:5000 vol/vol) (McCleland *et al.*, 2004) and anti-tubulin (1:2000 vol/vol; DM1A, Sigma). The hSpc25 antibody (Supplemental Figure 7) was chosen for its intensity and linearity. Horseradish peroxidase signal was detected with a FluoroChem FC2 imager (Alpha Innotech, now Cell Biosciences, Santa Clara, CA) and the signal intensity of each lane was measured using densitometry with FC2 software. Percent Ndc80^{bonsai} bound was determined by dividing the signal in the pellet sample by the 100% input control. GraphPad Prism software was used to determine if the binding data were best represented by a fitted curve with or without a Hill coefficient (h) by performing an extra sum-of-squares F test.

CD measurements

CD spectra of Hec1^{WT}, Hec1$^{\Delta N}$, and Hec1$^{K89E/K115E}$ Ndc80^{bonsai} proteins were collected in 10 mM Tris buffer, 100 mM NaCl, 1 mM

EDTA, 5% glycerol (pH 7.0) as previously described (Derewenda *et al.*, 2007).

Knockdown and rescue of Hec1/Ndc80 in HeLa cells

HeLa cells (American Type Culture Collection) were maintained in DMEM (Invitrogen) supplemented with 10% fetal bovine serum (Invitrogen) in a humidified incubator at 37°C with 5% CO_2. For synchronization, cells were seeded in medium containing 2 mM thymidine for 24 h, released into fresh medium for 12 h, arrested again in 2 mM thymidine for 12 h, released for 8–12 h, and fixed for immunofluorescence. Hec1/Ndc80 siRNA sequence and rescue sequence modifications were used as previously described (Miller *et al.*, 2008); however, CHD rescue constructs were expressed in the pEGFP-N1 vector. For knockdown and replacement experiments, cells were cotransfected at the first thymidine release with siRNA oligos and rescue plasmid using Lipofectamine 2000 (Invitrogen). Cells were transfected a second time with siRNA oligos at the second thymidine block using RNAiMax (Invitrogen). For mock and siRNA only controls, an empty pEGFP vector was used as the rescue plasmid. For CHD experiments, GAPD siRNA oligos (Thermo Scientific) were included as mock controls.

Immunofluorescence

Coverslips were cofixed and extracted in PHEM buffer (100 mM Pipes, pH 7.0, 10 mM Hepes, 10 mM EGTA, 2mM $MgCl_2$) containing 2% paraformaldehyde and 0.5% Triton X-100 for 20 min at room temperature. For cold lysis, cells were incubated on ice for 10–15 min in ice-cold medium before fixation with paraformaldehyde. Antibodies used were anti-Hec1/Ndc80 9G3 (1:500 [vol/vol]), anti-Spc25 (1:500 [vol/vol]) (McCleland *et al.*, 2004), anti–CENP-E (1:1000 [vol/vol]; a gift from Timothy Yen, Fox Chase Cancer Center, Philadelphia, PA), anti–KNL-1 (1:1000 [vol/vol]; a gift from Arshad Desai, UC San Diego, La Jolla, CA), anti-Mad2 (1:100 [vol/vol]; a gift from Gary Gorbsky, OMRF, Oklahoma City, OK), anti-BubR1 (1:500 [vol/vol]; BD Biosciences), anti-ACA (1:500 [vol/vol]; Antibodies Incorporated, Davis, CA), anti-tubulin (1:2000 [vol/vol]; DM1A; NeoMarkers, Freemont, CA) and fluorescein isothiocyanate (FITC)-conjugated anti-tubulin (1:500 [vol/vol]; DM1A; Sigma, St. Louis, MO). DAPI (4′,6-diamidino-2-phenylindole) staining (1:5000 [vol/vol] of a 5 mg/ml stock) was used to visualize DNA. Images in Supplemental Figures 3, 5, and 6 were captured by spinning disk confocal microscopy using either a 63× 1.4 NA or a 100× 1.4 NA Plan-Apochromatic Zeiss (Oberkochen, Germany) objective lens. A Zeiss Axiovert 200 inverted microscope was used with a Perkin Elmer-Cetus (Oberkochen, Germany) confocal attachment and a krypton/argon laser with AOTF control for detecting at 488, 568, and 647 nm. Digital images were obtained with a Hamamatsu (Bridgewater, NJ) digital CCD camera. Image acquisition, shutters, and z-slices were all controlled with UltraView RS imaging software (Perkin Elmer-Cetus). For Figures 1, 2, 3, and 4, images were collected using a 100× lens on a DeltaVision microscope (Applied Precision, Issaquah, WA) and deconvolved z-projections are shown. Interkinetochore distance measurements and relative Hec1/Ndc80 intensity levels were quantified using softWoRx imaging software (Applied Precision).

Hec1/Ndc80 intensity levels

Hec1/Ndc80 9G3 antibody was used to stain cells in the 568-nm channel to allow comparison across mock, $Hec1^{WT}$, and $Hec1^{K89E/K166E}$ conditions. Hec1/Ndc80 intensity was quantified by calculating kinetochore fluorescence in a square 9×9 pixel area and subtracting out background from the surrounding 13×13 pixel area as previously described (Hoffman *et al.*, 2001).

ACKNOWLEDGMENTS

We thank Dan Burke and Dan Foltz for critical reading of the manuscript. We also thank members of the Stukenberg lab, especially Pawel Janczyk, for helpful comments and discussions, and we thank members of the Foltz lab for their ongoing generosity. Finally, we are grateful to Andrea Musacchio ($Ndc80^{bonsai}$ constructs), Gary Gorbsky (Mad2 antibody), Arshad Desai (KNL-1 antibody), and Tim Yen (CENP-E antibody) for providing reagents. J.G.T. was supported by the Cancer Training Grant from the University of Virginia; S.A.M. was supported by the Cell and Molecular Biology Training Grant from the University of Virginia. This work was funded by the National Institutes of Health (1RO1GM081576).

REFERENCES

Alushin GM, Ramey VH, Pasqualato S, Ball DA, Grigorieff N, Musacchio A, Nogales E (2010). The Ndc80 kinetochore complex forms oligomeric arrays along microtubules. Nature 467, 805–810.

Brinkley BR, Cartwright J Jr (1975). Cold-labile and cold-stable microtubules in the mitotic spindle of mammalian cells. Ann N Y Acad Sci 253, 428–439.

Cheeseman IM, Chappie JS, Wilson-Kubalek EM, Desai A (2006). The conserved KMN network constitutes the core microtubule-binding site of the kinetochore. Cell 127, 983–997.

Cheeseman IM, Desai A (2008). Molular architecture of the kinetochore-microtubule interface. Nat Rev Mol Cell Biol 9, 33–46.

Ciferri C *et al.* (2008). Implications for kinetochore-microtubule attachment from the structure of an engineered Ndc80 complex. Cell 133, 427–439.

Cleveland DW, Mao Y, Sullivan KF (2003). Centromeres and kinetochores: from epigenetics to mitotic checkpoint signaling. Cell 112, 407–421.

Deluca JG, Gall WE, Ciferri C, Cimini D, Musacchio A, Salmon ED (2006). Kinetochore microtubule dynamics and attachment stability are regulated by Hec1. Cell 127, 969–982.

Deluca JG, Howell BJ, Canman JC, Hickey JM, Fang G, Salmon ED (2003). Nuf2 and Hec1 are required for retention of the checkpoint proteins Mad1 and Mad2 to kinetochores. Curr Biol 13, 2103–2109.

Deluca JG, Moree B, Hickey JM, Kilmartin JV, Salmon ED (2002). hNuf2 inhibition blocks stable kinetochore-microtubule attachment and induces mitotic cell death in HeLa cells. J Cell Biol 159, 549–555.

Derewenda U *et al.* (2007). The structure of the coiled-coil domain of Ndel1 and the basis of its interaction with Lis1, the causal protein of Miller-Dieker lissencephaly. Structure 15, 1467–1481.

Desai A, Murray A, Mitchison TJ, Walczak CE (1999). The use of Xenopus egg extracts to study mitotic spindle assembly and function in vitro. Methods Cell Biol 61, 385–412.

Du J *et al.* (2008). The mitotic checkpoint kinase NEK2A regulates kinetochore microtubule attachment stability. Oncogene 27, 4107–4114.

Guimaraes GJ, Dong Y, McEwen BF, Deluca JG (2008). Kinetochore-microtubule attachment relies on the disordered N-terminal tail domain of Hec1. Curr Biol 18, 1778–1784.

Hayashi I, Ikura M (2003). Crystal structure of the amino-terminal microtubule-binding domain of end-binding protein 1 (EB1). J Biol Chem 278, 36430–36434.

Hiser L, Aggarwal A, Young R, Frankfurter A, Spano A, Correia JJ, Lobert S (2006). Comparison of beta-tubulin mRNA and protein levels in 12 human cancer cell lines. Cell Motil Cytoskeleton 63, 41–52.

Hoffman DB, Pearson CG, Yen TJ, Howell BJ, Salmon ED (2001). Microtubule-dependent changes in assembly of microtubule motor proteins and mitotic spindle checkpoint proteins at PtK1 kinetochores. Mol Biol Cell 12, 1995–2009.

Maddox P, Straight A, Coughlin P, Mitchison TJ, Salmon ED (2003). Direct observation of microtubule dynamics at kinetochores in Xenopus extract spindles: implications for spindle mechanics. J Cell Biol 162, 377–382.

Maiolica A, Cittaro D, Borsotti D, Sennels L, Ciferri C, Tarricone C, Musacchio A, Rappsilber J (2007). Structural analysis of multiprotein complexes by cross-linking, mass spectrometry, and database searching. Mol Cell Proteomics 6, 2200–2211.

Martin-Lluesma S, Stucke VM, Nigg EA (2002). Role of Hec1 in spindle checkpoint signaling and kinetochore recruitment of Mad1/Mad2. Science 297, 2267–2270.

McCleland ML, Gardner RD, Kallio MJ, Daum JR, Gorbsky GJ, Burke DJ, Stukenberg PT (2003). The highly conserved Ndc80 complex is required for kinetochore assembly, chromosome congression, and spindle checkpoint activity. Genes Dev 17, 101–114.

McCleland ML, Kallio MJ, Barrett-Wilt GA, Kestner CA, Shabanowitz J, Hunt DF, Gorbsky GJ, Stukenberg PT (2004). The vertebrate Ndc80 complex contains Spc24 and Spc25 homologs, which are required to establish and maintain kinetochore-microtubule attachment. Curr Biol 14, 131–137.

Miller SA, Johnson ML, Stukenberg PT (2008). Kinetochore attachments require an interaction between unstructured tails on microtubules and Ndc80(Hec1). Curr Biol 18, 1785–1791.

Powers AF, Franck AD, Gestaut DR, Cooper J, Gracyzk B, Wei RR, Wordeman L, Davis TN, Asbury CL (2009). The Ndc80 kinetochore complex forms load-bearing attachments to dynamic microtubule tips via biased diffusion. Cell 136, 865–875.

Santaguida S, Musacchio A (2009). The life and miracles of kinetochores. EMBO J 28, 2511–2531.

Sjoblom B, Ylanne J, Djinovic-Carugo K (2008). Novel structural insights into F-actin-binding and novel functions of calponin homology domains. Curr Opin Struct Biol 18, 702–708.

Slep KC, Vale RD (2007). Structural basis of microtubule plus end tracking by XMAP215, CLIP-170, and EB1. Mol Cell 27, 976–991.

Wan X *et al.* (2009). Protein architecture of the human kinetochore microtubule attachment site. Cell 137, 672–684.

Wei RR, Al Bassam J, Harrison SC (2007). The Ndc80/HEC1 complex is a contact point for kinetochore-microtubule attachment. Nat Struct Mol Biol 14, 54–59.

Wei RR, Schnell JR, Larsen NA, Sorger PK, Chou JJ, Harrison SC (2006). Structure of a central component of the yeast kinetochore: the Spc24p/Spc25p globular domain. Structure 14, 1003–1009.

Wei RR, Sorger PK, Harrison SC (2005). Molecular organization of the Ndc80 complex, an essential kinetochore component. Proc Natl Acad Sci USA 102, 5363–5367.

Welburn JP, Vleugel M, Liu D, Yates JR III, Lampson MA, Fukagawa T, Cheeseman IM (2010). Aurora B phosphorylates spatially distinct targets to differentially regulate the kinetochore-microtubule interface. Mol Cell 38, 383–392.

Wigge PA, Kilmartin JV (2001). The Ndc80p complex from Saccharomyces cerevisiae contains conserved centromere components and has a function in chromosome segregation. J Cell Biol 152, 349–360.

Zimniak T, Stengl K, Mechtler K, Westermann S (2009). Phosphoregulation of the budding yeast EB1 homologue Bim1p by Aurora/Ipl1p. J Cell Biol 186, 379–391.